



GAMMA-2, Scientific Workshop on the Emission of Prompt Fission Gamma-Rays in Fission and Related Topics

## Prompt $\gamma$ -rays from the fast neutron induced fission on $^{235,238}\text{U}$ and $^{232}\text{Th}$

M.Lebois<sup>a,\*</sup>, J.N. Wilson<sup>a</sup>, P. Halipré<sup>a</sup>, B. Leniau<sup>a</sup>, I. Matea<sup>a</sup>, A. Oberstedt<sup>b,c</sup>, S.Oberstedt<sup>d</sup>, D. Verney<sup>a</sup>

<sup>a</sup>*Institut de Physique Nucléaire d'Orsay, CNRS/Univ. Paris Sud-XI, 91406 Orsay Cedex, France*

<sup>b</sup>*CEA/DAM Ile-de-France, 91297 Arpaçon Cedex, France*

<sup>c</sup>*Fundamental Physics, Chalmers University of Technology, 41296 Göteborg, Sweden*

<sup>d</sup>*European Commission, DG Joint Research Centre (IRMM), 2440 Geel, Belgium*

### Abstract

Preliminary results from the first experiment using the LICORNE neutron source at the IPN Orsay are presented. Prompt fission gamma rays from fast-neutron induced fission of  $^{238}\text{U}$ ,  $^{232}\text{Th}$  and  $^{235}\text{U}$  were detected. Thick samples of around 50g of  $^{238}\text{U}$  and  $^{232}\text{Th}$  are used for the first part of the experiment. An ionisation chamber containing  $\sim 10$  mg samples of  $^{238}\text{U}$  and  $^{235}\text{U}$  to provide a fission trigger is used for the second part of the experiment. Gamma rays have been detected using 17 high efficiency  $\text{BaF}_2$  detectors and 6  $\text{LaBr}_3$  scintillator detectors.

© 2014 Published by Elsevier B.V. This is an open access article under the CC BY-NC-ND license

(<http://creativecommons.org/licenses/by-nc-nd/3.0/>).

Selection and peer-review under responsibility of Guest Editor: Mr. Stephan Oberstedt - [stephan.oberstedt@ec.europa.eu](mailto:stephan.oberstedt@ec.europa.eu)

**Keywords:** fast neutron; fission; prompt gamma rays; LICORNE

### 1. Introduction

In a reactor core the major nuclear reaction is fission. It is the origin of the majority of the power released. During the fission process,  $\gamma$ -rays and neutrons are released. Due to the reactor design,  $\gamma$ -rays have an average mean free path greater than neutrons (tenth of centimeters) and then can carry, far from the initial reaction site, roughly 10% of the energy released in the process. During reactor operation, gamma heating process dominates in all non-fissile materials in the reactor core – e.g. structural materials, core shielding, reactor instrumentation, etc. Then, calculation of reactor core temperatures becomes a difficult problem. When the reactor is shut down, gamma heating is the dominant energy deposition process for all core materials and thus the problem of gamma heating is directly related to reactor safety. Currently, benchmark models of gamma heating in reactor cores underestimate heating effects by up to 30% when compared to experimental results (Rimpault, 2005). This is mainly due to insufficiently accurate nuclear data and possibly also deficiencies in the modeling. The gamma rays originating from neutron capture, inelastic scattering and beta decay of the fission fragments are fairly well understood. However, about 40% of this energy

*E-mail address:* [lebois@ipno.in2p3.fr](mailto:lebois@ipno.in2p3.fr)

\* Corresponding author. Tel.: +33-169-157-429 ; fax: +33-169-156-470.

is prompt gamma emission ( $< 1$  ns) and here, the available data for thermal neutron induced fission date from the early 1970's (Verbinski et al., 1973; Pelle et al., 1971). However, these data have the potential for improvement and such measurements are at the top of the high priority nuclear data list of the NEA/OECD (NEA, 2006). Since future generation IV reactor concepts will mostly use fast neutron spectra, prompt  $\gamma$  emission data in fast neutron induced fission are very important. However, currently very little data of this kind exists. For fast neutron induced fission the spectral shape, mean multiplicities and energies are expected to be different because excitation energy and angular momentum of the fissioning compound nucleus will change, along with the resulting fission yields, average neutron energies and multiplicities. There are particular technical challenges associated with prompt  $\gamma$ -ray emission measurements for fast neutron induced fission. Firstly, fission cross sections are typically three orders of magnitude lower than those for thermal neutron induced fission. To produce high fluxes the target and  $\gamma$  detectors need to be very close to the neutron source. However, since conventional quasi mono-energetic neutron sources emit neutrons isotropically  $\gamma$  detectors will require heavy shielding to avoid being blinded by neutrons from the source, which is often highly impractical – a problem that LICORNE has now solved.

## 2. Experimental Measurement

A first experiment using LICORNE was conducted in July 2013 over a period of two weeks to measure prompt fission  $\gamma$  ray spectra of  $^{232}\text{Th}$ ,  $^{238}\text{U}$ ,  $^{235}\text{U}$  and  $^{252}\text{Cf}$ . The experiment was financed by ERINDA and was split into two parts with around 100 h of beam time allocated to each part.

### 2.1. Fission tag with an ionisation chamber

The first part used a cylindrical twin Frisch grid ionization chamber of 28 cm diameter and 20 cm length. The chamber was filled with P10 counting gas (90% argon, 10% methane) to detect fission fragments with an efficiency of almost 100%. Two targets of  $^{235}\text{U}$  and  $^{238}\text{U}$  were placed back to back at the central cathode position and signals from the cathode and anode were digitized and recorded to disk. The targets consisted of approximately 10 mg of uranium, forming circular deposits of 6.5 cm diameter on aluminium backings of 30  $\mu\text{m}$  thickness. Fission fragments emitted from the surface of the targets were identified by measuring the anode and cathode signals in coincidence and placing a constraint on the minimum pulse heights recorded to reject intrinsic alpha activity. For  $\gamma$  detection 14 hexagonal  $\text{BaF}_2$  scintillator crystals were configured into two independent clusters of seven detectors. Each crystal measured 10 cm diameter and 14 cm in length for a total mass of scintillator of 62 kg. The two clusters were placed at 29 cm from the target position at angles of  $\pm 62$  degrees to the beam axis. In such a configuration, the total geometric efficiency of the two clusters was estimated to be 7%. MCNP simulations of the clusters and targets show that each cluster has a high photo-peak efficiency of 2.1% and a peak-to-total ratio of 75% for  $\gamma$ -rays of energy 1 MeV. Figure 1 shows a schematic diagram of the setup for the first part of the experiment.

Neutrons of average energy 1.5 MeV from the LICORNE inverse kinematics neutron source were used to bombard the targets with estimated fluxes at the target position of up to  $2 \times 10^5$  n/s/cm<sup>2</sup>. This gave maximum fission rates of around 0.3 fissions per second and 1.2 fissions per second for  $^{238}\text{U}$  and  $^{235}\text{U}$  targets respectively. In total  $4.2 \times 10^4$  fission events of  $^{238}\text{U}$  and  $1.5 \times 10^5$  fission events for  $^{235}\text{U}$  were recorded to disk over a period of around 3 days. The data acquisition system is based on a triggerless COMET-6X (COdage et Marquage En Temps) module that allows us to encode in amplitude the signals delivered by up to 6 detectors per module with a capacity to chain five modules together, and to associate with each amplitude encoding an absolute and high resolution (400 ps) time information.

### 2.2. Fission tag with $\text{BaF}_2$ clusters

The second part of the experiment involved the same two clusters of 14  $\text{BaF}_2$  in a close packed geometry around thick samples (replacing the ionization chamber) of  $^{238}\text{U}$  (38 g) and  $^{232}\text{Th}$  (50 g), forming a calorimeter with a geometric efficiency of approximately 70%. The  $^{238}\text{U}$  sample was a disc of 6.5 cm diameter and the thorium sample a square of dimensions 5 cm  $\times$  5 cm. The cone of neutrons was produced from a  $^7\text{Li}$  beam of 15 MeV bombarding energy was emitted at a maximum opening angle of 20 degrees and passed through the centre of the calorimeter to

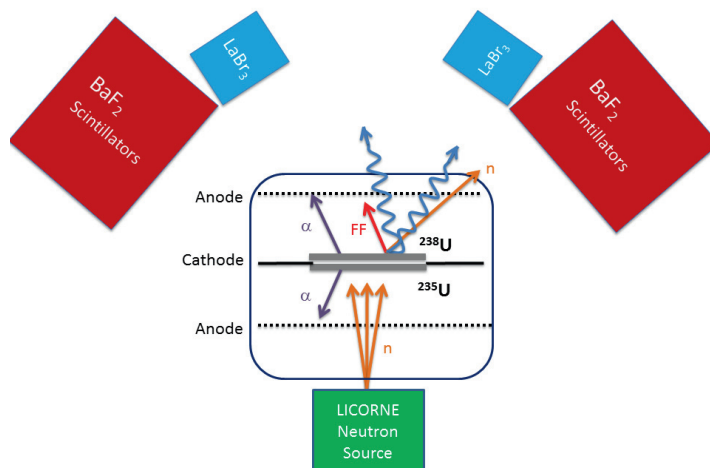


Fig. 1. Schematic diagram of the experimental setup for the first part of the experiment with an ionization chamber

irradiate the thick samples placed at 14 cm from the neutron source. It was estimated that fission rates of 500 and 150 fissions per second were produced in the  $^{238}\text{U}$  and  $^{235}\text{U}$  samples respectively. Neutron beams were pulsed at 2.5 MHz rate (400 ns between bunches) and bunch width of around 2 ns. This allowed timing information from the beam buncher to be used as a reference with which to measure event detection times relative to the bunch. Fission events can be discriminated from background by looking for high sum-energy and multiplicity events in the calorimeter that occurred within a short time window. The background is complex and arises from several sources:  $^7\text{Li} + ^{12}\text{C}$  fusion evaporation reactions in the polypropylene giving rise to high energy  $\gamma$ -rays and neutrons, intrinsic activity of the target itself, parasitic neutrons from the  $^7\text{Li} + ^{12}\text{C}$  reactions provoking  $(n,n')$  reactions in the scintillators,  $(n,n')$  reactions in the detectors from scattering of the primary neutron beam on the target, intrinsic activity of the scintillator crystals, and  $\gamma$ 's from the room. Once fission events are identified, the spectrum in coincidence of  $\text{LaBr}_3$  detectors can be projected.

### 3. Data Analysis

#### 3.1. Preliminary Analysis for the first part of the experiment

The important step in the data analysis for this part of experiment was to find the time correlations between fission events in the ionization chamber and coincident  $\gamma$ -rays in one of the surrounding detectors. The ionization chamber contained two targets and we considered two types of events. One was based on a coincidence of cathode and anode for the  $^{238}\text{U}$  side of the chamber. The other was based on a cathode/anode coincidence for the  $^{235}\text{U}$  side. After selection of the fission events coincident  $\gamma$ -rays in the  $\text{BaF}_2$  or  $\text{LaBr}_3$  were put in a histogram. The figure 2a. represent the 2 dimensional graph obtained for the coincidences between cathode and  $^{238}\text{U}$  anode with a time window of 500 ns. The intrinsic  $\alpha$  activity of the target can be observed – in the lower left corner – for small amplitude on both channels. Fission fragments can be easily recognized since their mass and kinetic energy are high they produce a large amplitude signal on both cathode and anode. Events along the diagonal are identified as fission events. During the experiment we observed a saturation on the cathode, which explains why all the events are not on the diagonal. However, this effect will be corrected offline in the near future. After the selection of fission fragments, time correlation between cathode event and a  $\gamma$  detector hit were reconstructed. Time of flight can then be calculated as a function of the measured  $\gamma$ -ray energy as shown on figure 2b. In the center of this matrix a horizontal line can be observed which corresponds

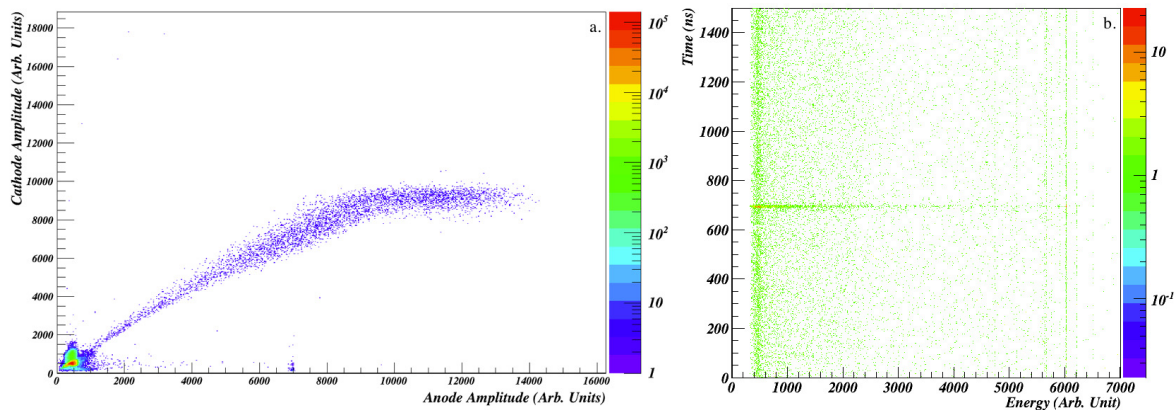


Fig. 2. On the left: 2 dimensional histogram showing the coincidences between cathode and anode for the  $^{238}\text{U}$  target. On the right: time difference between a cathode and a  $\gamma$  event as a function of the measured  $\gamma$ -ray energy.

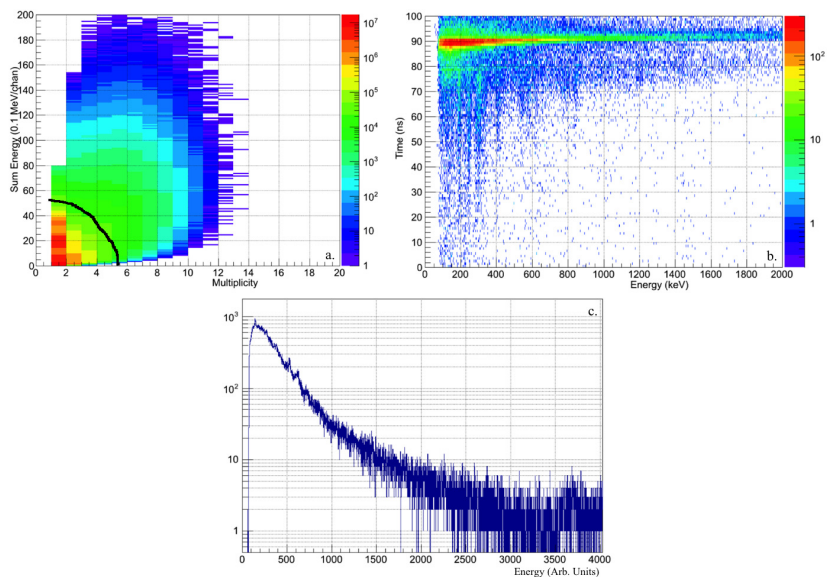


Fig. 3. Picture a: Total energy as a function of the  $\gamma$  multiplicity in the  $\text{BaF}_2$  crystals. Picture b: Time between a fission event tagged with  $\text{BaF}_2$  and a  $\gamma$ -ray detected in the  $\text{LaBr}_3$  crystal versus the  $\gamma$ -ray energy. Picture c: Raw prompt fission gamma spectrum measured for  $^{252}\text{Cf}$  without deconvolution of the detector response.

to the prompt fission  $\gamma$ -rays. These results are only preliminary and represent just a small fraction of the whole data set. Further work must be performed to obtain the final prompt  $\gamma$  spectrum such as performing the same procedure for the LaBr<sub>3</sub> detectors and deconvoluting detector response from the experimental data. However, these preliminary results are encouraging.

### 3.2. Demonstration of principle with the <sup>252</sup>Cf source

In the second part of the experiment, the major difficulty is how to recognize a fission event *via* an indirect gamma-ray sum energy and multiplicity tag. The BaF<sub>2</sub> detectors are exposed to a complex background from secondary neutrons and gammas, the intrinsic activity of the target materials and the intrinsic activity of the detectors themselves. However, these background events all have low multiplicities ( $\leq 2$ ). In contrast, the fission process releases typically 8  $\gamma$ -rays on average. High multiplicity events ( $\geq 3$ ) can thus be exploited to tag fission. Furthermore, the fission process releases up to 20 MeV *via* gamma emission. Thus the total energy measured in the BaF<sub>2</sub> cluster will be greater than the amount of energy deposited by (n,n') events with 4 MeV neutrons.

This selection technique has been demonstrated to work well for a <sup>252</sup>Cf source in circumstances where the relative background is quite low. Figure 3a. shows the 2D histogram of the multiplicity and sum energy of events detected in the calorimeter. The fission events are selected to the right of the black line, eliminating backgrounds from intrinsic activity of the BaF<sub>2</sub> detectors and the room. Then, the fission event time is clearly determined and it is possible to obtain the time of flight from the target to an LaBr<sub>3</sub> detector as shown on figure 3b. . There are two major components in this graph. First, the horizontal line around 90 ns corresponds to the prompt fission gamma rays. Just below this line at later times structures appear. These are caused by prompt fission neutrons interacting with the detectors *via* (n,n') reactions. The vertical lines at lower energy are caused by the slowest neutrons that induce (n,n') reactions on the lowest lying states in La and Br nuclei. Figure 3c. is produced by projecting the prompt line at 90 +/- 3 ns on the X-axis. However, this is the raw spectrum and cannot be directly compared to those in the literature (Laborie et al., 2012) since no deconvolution of the detector response has yet been performed. Extensive studies about the influence of the cut in fig. 3a. need to be performed to test whether a bias is introduced into the spectrum. However, the general shape of this spectrum is similar to that shown in (Laborie et al., 2012). In the future, this technique will be applied to the <sup>238</sup>U and <sup>232</sup>Th data.

## 4. Conclusion

The measurement of prompt  $\gamma$ -rays from fast neutron induced fission for <sup>238</sup>U, <sup>235</sup>U and <sup>232</sup>Th was the first experiment carried out using the LICORNE neutron source. The focused neutron beam allowed BaF<sub>2</sub> and LaBr<sub>3</sub> gamma detectors to be placed in a very close geometry to the actinide sample and were not blinded by the neutrons from the source. This is a completely new experimental technique for the spectroscopy of neutron induced reactions. The experiment was performed over 200 hours of beam time and approximately 1 Tb of data were acquired. A new method to tag the fission was tested and validated with a <sup>252</sup>Cf, but now needs to be applied to the experiment data under conditions of much higher background. The data analysis is ongoing but is already producing some encouraging results.

## References

- Laborie, J.M., Belier, G., and Taieb, J., Phys. Proc. 31 (2012) 13.
- NEA nuclear data high priority request list, <http://www.oecd-neo.org/dbdata/hprl> nea.org/dbdata/hprl.
- Pelle, R.W., and Maienschein, F.C., Phys. Rev. C3, 373 (1971).
- Rimpault, G., Proceedings of the workshop on nuclear data needs for generation IV, Antwerp, Belgium World Scientific ISBN 981-256-830-1 (2005) 46.
- Verbinski, V.V., Weber, H., and Sund, R.E., Phys. Rev. C7, 1173 (1973).